Pageoph, Vol. 115 (1977), Birkhäuser Verlag, Basel

The Stress State Near Spanish Peaks, Colorado Determined From a Dike Pattern

By OTTO H. MULLER[1]) and DAVID D. POLLARD[2])

Abstract – The radial pattern of syenite and syenodiorite dikes of the Spanish Peaks region is analysed using theories of elasticity and dike emplacement. The three basic components of Odé's model for the dike pattern (a pressurized, circular hole; a rigid, planar boundary; and uniform regional stresses) are adopted, but modified to free the regional stresses from the constraint of being orthogonal to the rigid boundary. Dike areal density, the White Peaks intrusion, the strike of the upturned Mesozoic strata, and the contact between these strata and the intensely folded and faulted Paleozoic rocks are used to orient the rigid boundary along a north–south line. The line of dike terminations locates the rigid boundary about 8 km west of West Peak. The location of a circular plug, Goemmer Butte, is chosen as a point of isotropic stress. A map correlating the location of isotropic stress points with regional stress parameters is derived from the theory and used to determine a regional stress orientation (N82E) and a normalized stress magnitude. The stress trajectory map constructed using these parameters mimics the dike pattern exceptionally well. The model indicates that the regional principal stress difference was less than 0.05 times the driving pressure in the West Peak intrusion. The regional stress difference probably did not exceed 5 MN/m^2.

Key words: Stress field regional; Volcanic dike pattern; Paleopiezometer.

1. Introduction

The geology of the Spanish Peaks region and the petrology of its igneous rocks have been described by ENDLICH (1878), HILLS (1901), KNOPF (1936), and JOHNSON (1960, 1961, 1968). Sedimentary rocks of the Raton basin, which range in age from Cretaceous to Eocene and are predominantly shales, sandstones, and conglomerates, form the broad asymmetric La Veta syncline (Fig. 1a). The steep western limb of the syncline abuts the intensely folded and faulted Paleozoic rocks of the Sangre de Cristo Mountains, while the eastern limb merges into the horizontal strata of the plains. Two prominent topographic features, West and East Spanish Peak, are about 11 km and 15 km east of the Paleozoic–Mesozoic contact and rise almost 2 km above the surrounding plains. The peaks are composed predominantly of igneous rock as well as some metamorphosed and deformed sedimentary rock. The principal intrusive form associated with each peak is described by Johnson as a stock. The rocks of the peaks, being more resistant to weathering and erosion than the surrounding sedimentary rocks, produce the dramatic relief. Numerous nearly vertical dikes crop

[1]) Colgate University, Hamilton, New York 13346.
[2]) U.S. Geological Survey, Menlo Park, California 94025.

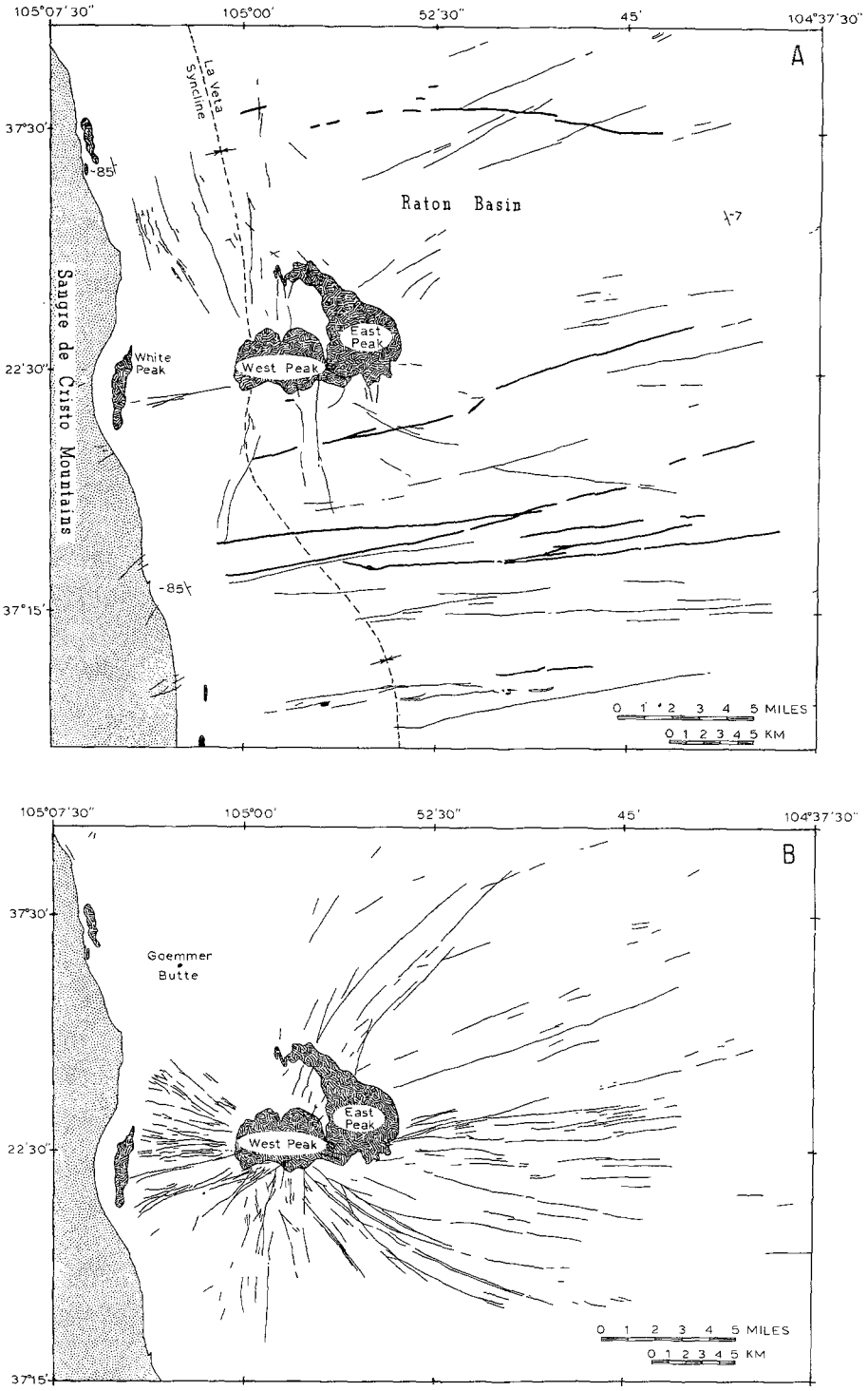

Figure 1

Maps of dikes (solid lines) in the Spanish Peaks region of south central Colorado. Stippled pattern is intensely folded and faulted Paleozoic rock. Hatched pattern is igneous rock. From JOHNSON (1968). (A) Dikes present in Johnson's 1968 map, but not used in our analysis. Thicker lines are syenodiorite dikes of the subparallel swarm. Thinner lines are dikes having compositions other than syenite or syenodiorite. (B) Syenite and syenodiorite dikes used in our analysis.

out around the peaks and some of these form a radial pattern focused approximately on West Peak (Fig. 1b).

The pattern formed by the intersection of the ground surface and these dikes (i.e., the map pattern) was the subject of papers by ODÉ (1957) and JOHNSON (1961). Odé pointed out the similarity between the pattern of maximum principal stress trajectories for a particular elasticity theory model, and the dike pattern as mapped by KNOPF (1936). Odé used all of the dikes on Knopf's map regardless of petrology or orientation. His model consisted of a pressurized circular hole adjacent to a rigid, planar boundary in a two dimensional elastic plate. On this stress system he superimposed a homogeneous far field stress having principal stresses parallel and perpendicular to the rigid boundary. The hole was believed analogous to West Peak stock, the rigid boundary represented the Sangre de Cristo mountain front (i.e., the Paleozoic–Mesozoic contact), and the far field stresses accounted for the regional stress state in the horizontal plane at the time of intrusion. Odé's work suggests that the dikes were emplaced along stress trajectories having orientations which were locally controlled by the stock and Sangre de Cristo range, while far from these features the dikes curved into the trend of the maximum principal regional stress. This work has been cited in several textbooks as an excellent example of the application of theoretical work to structural problems in geology (HILLS, 1963, pp. 377–380; A. JOHNSON, 1970, pp. 400–428). We agree with these citations, but suggest that further development of the model is warranted in light of recent geologic work in the region.

JOHNSON (1961, 1968) presented a new map of the igneous rocks and separated the dikes on a geometric basis into a radial set and a subparallel set trending roughly east–west. We presume that the subparallel set is not related to West Peak and should therefore be excluded from the analysis of the radial pattern. Johnson's map includes many radial dikes not on Knopf's map, particularly to the west of West Peak, which should be included in the analysis. Because none of the radial dikes contact the stock and many are discontinuous along their outcrop trend, Johnson argued that the magma intruded from below the present erosion surface. This contention is supported by SMITH (1975), who used elongated vesicles, and by POLLARD *et al.* (1975), who used contact offsets, to suggest an upward and outward propagation direction for some of the dikes. On the basis of the diverse petrology of different dikes and their cross-cutting relationships, Johnson delineated several (at least seven) different magmatic phases. We cannot justify the assumption that the same stress field existed during all of these phases. Johnson also suggested that the dikes selectively intruded along joints that formed prior to igneous activity. These new field data and interpretations may cause some readers to question the appropriateness of Odé's stress analysis. However, we present arguments below which support the continued use of the basic components of the analysis.

Our first objective is to review the basic postulates of the theory and discuss its applicability to the origin of the dike pattern. Next we modify the model of Odé to

account for an arbitrary orientation of the far field stresses and point out some new deductions from this model. Geologic criteria based in part upon Johnson's map are used to select dikes for analysis and to fix the model parameters which are used to derive a trajectory pattern. Finally, we interpret the pattern of selected dikes in the Spanish Peaks region in light of the modified model and present a stress field which accounts for the dike pattern.

2. Evaluation of the Theory

For the purpose of discussion we will briefly review the fundamental postulates of elasticity theory without presenting the governing equations which may be found in standard texts (TIMOSHENKO and GOODIER, 1951; MUSKHELISHVILI, 1975). In formulating the two dimensional differential equations of equilibrium for stresses and of compatibility for strains and displacements, one postulates that the model is a static continuum. A linear relation between stress and strain is postulated and the 21 independent elastic constants of the generalized Hooke's Law are reduced to two familiar elastic moduli (Young's modulus; Poisson's ratio) by postulating the model is homogeneous and isotropic with respect to these moduli. The resulting stress-strain equations can be modified further by postulating conditions of plane strain or generalized plane stress and the result used to write the compatibility equation in terms of stresses. Then, neglecting body forces in the plane of interest, the equilibrium and compatibility equations are combined to derive the biharmonic differential equation for the Airy stress function. This equation must be satisfied along with the boundary conditions to find a suitable solution for a particular problem.

Upon first comparing the model postulates with the complexity of the geology in the Spanish Peaks region, it may seem remarkable that a good correlation exists between the stress trajectory pattern derived by Odé and the dike pattern on the map of Knopf. We have insufficient data on the rock properties and physical conditions at the time of intrusion to evaluate differences between the idealized model and the real situation precisely, but we feel that a qualitative evaluation is necessary.

In order to compare the dike pattern with a stress trajectory pattern, we need not resolve stresses within areas less than about 1 km^2. On this scale a horizontal slab of the earth's crust does not contain voids which would make the continuum model inappropriate. Because of the relatively great magma viscosity and small driving pressures, we conclude that inertial forces related to intrusion were negligible and a static model is appropriate. Temperatures and confining pressures in the upper 5 km of the crust over most of the Spanish Peaks region probably did not exceed 250°C and 150 MN/m^2. Under such conditions many sedimentary rocks are adequately described as linear elastic materials (HANDIN, 1966). Within several kilometers of the West Peak intrusive complex or within several meters of the periphery of advancing dikes, elevated temperatures and large differential stresses resulted in nonlinear and irrecoverable deformation not described by the model.

Lithologic variation in the sedimentary rock of the Spanish Peaks region forms a distinct geologic inhomogeneity which may also represent a mechanical inhomogeneity. For clastic sedimentary rock, Young's modulus varies from 6×10^{10} to 10^{12} N/m^2 and Poisson's ratio varies from 0.03 to 0.3 (BIRCH, 1966). The ranges of these moduli over much of the Raton Basin were probably smaller because the strata are nearly horizontal (sub-parallel to the plane of the model) and have similar histories of compaction, cementation, and deformation. Another geologic inhomogeneity exists west of West Peak, where the strata of the Raton Basin are abruptly upturned, thrust faulted, and juxtaposed against the intensely folded and faulted rocks of the Sangre de Cristo mountains. The dike pattern was apparently influenced by one or more of these structures because dikes extend less than 10 km to the west, but up to 30 km to the east of the peak. The model treats this inhomogeneity by imposing special boundary conditions along a line paralleling the trend of these structures. Any differences in elastic moduli between rocks on either side of this line are not accounted for directly, but rather through the choice of boundary conditions.

The possibility of significant directional dependency (anisotropy) of elastic moduli is minimized by considering a horizontal slab which is sub-parallel to strata over much of the region. The rocks do contain tectonic joints; however, a joint pattern described by JOHNSON (1961) as complex, perhaps random, may not produce a significant anisotropy. Locally a dike might propagate along a joint, but it would tend to select joints oriented parallel to the maximum principal stress. A significant moduli anisotropy in the horizontal plane may exist in the upturned beds west of West Peak; however, its effect is treated by the boundary conditions.

A two dimensional analysis is justified in that most dikes of the region are nearly vertical and some can be traced over a 1 km change in elevation (JOHNSON, 1961). We represent the stock by a vertical cylindrical body although little supportive evidence is available. Choice between a plane strain or generalized plane stress case is not clear cut. The plane stress case may be a good description of conditions near the ground surface, but probably does not apply at depth. Near the mid-depth of the intrusive structures the plane strain case should provide a reasonable description of natural conditions, but it does not apply near the ground surface. Nevertheless, the in-plane stress distribution and stress trajectories are identical for both plane stress and plane strain. The stress state is independent of elastic moduli if the in-plane body forces are constant or zero, a likely condition for a horizontal plane.

The postulates of sheet intrusion theory also must be examined. ANDERSON (1938, 1972) proposed that the wedging effect of magma in dikes will be greatest along fissures which are perpendicular to the 'smallest rock pressure,' and that these fissures will offer the 'least resistance' to intrusion of the magma. STEVENS (1911) made a similar proposal. The above statements are easily corroborated, if one accepts a very eccentric, pressurized elliptical hole in a two dimensional elastic body as a good model for a dike; one interprets 'smallest rock pressure' to mean least principal far field stress; and one specifies uniform far field stresses (POLLARD, 1973). The tensile

stress (wedging action) acting across the end of the long axis of the hole is maximized when the length of the hole is perpendicular to the minimum principal far field stress. Also, a given dilation of the hole is accomplished by the least internal pressure (least resistance) with this geometrical arrangement. Because of symmetry, one trajectory of maximum principal stress extends from the ends of the hole parallel to its long axis. Upon tensile failure, the hole should propagate along this trajectory maintaining a linear form.

The situation for the Spanish Peaks dikes is more complex than this simple model for a single dike. Because a uniform regional stress field is believed to have been perturbed by the stock and mountain front prior to dike intrusion, stress trajectories were not straight lines. How a dike would respond to such a non-uniform stress field is not known, but several studies bear on the problem. Theoretical work by ERDOGAN and SIH (1963), POLLARD (1973), and SIH (1974) suggest that if the maximum principal far field stress is not parallel to the dike, the initial propagation direction should be out of the original plane of the dike and generally toward the direction of maximum far field stress. Experiments by BRACE and BOMBOLAKIS (1963). ERDOGAN and SIH (1963), and HOEK and BIENIAWSKI (1965) confirm these tendencies. Thus a qualitative argument can be made that in a non-uniform stress field a dike should adjust its course of propagation to follow a maximum principal stress trajectory. This adjustment may result in the division of a dike into closely-spaced, *en echelon* segments (POLLARD *et al*, 1975). Such details of dike form are ignored in this analysis although SMITH (1975) has clearly shown that many dikes south-east of West Peak are made up of *en echelon* segments. We use only the general trend of dikes as mapped by JOHNSON (1968).

We will propose a single stress trajectory pattern to compare with the dike pattern. However, a detailed analysis by SMITH (1975) identified two foci for radial dikes south-east of West Peak. In addition, emplacement of a dike may modify the original stress field up to distances of about twice the dike length (POLLARD, 1973). The discontinuous nature of dikes would reduce the area of stress modification, still, after several dikes intruded near West Peak, we would expect the original stress pattern to have changed, and we would not expect the closely-spaced dikes to follow a unique pattern of trajectories. The good correlation between dikes and trajectories found by Odé leads us to suggest that the region around the peak continued to feel the effects of the original stress field while stresses induced by each dike relaxed. The pattern of dikes seems to reflect this unique stress field due to the stock, boundary, and regional stresses without significant alteration by dike intrusion or movement of the focus.

Geologic evidence indicates that dike propagation was not restricted to a horizontal plane. Dikes probably intruded upward and outward from the West Peak area through the horizontal section considered by the model. Because dikes are nearly vertical over 1 km depths, we conclude that the horizontal stress trajectories did not vary substantially over this depth. Thus, the fact that propagation was not horizontal is not a substantive criticism of the model.

3. Derivation of the Model

The model combines the several solutions suggested by Odé and having parameters shown in Fig. 2. Solutions are presented in terms of Airy stress functions which may be differentiated to derive the stress field (TIMOSHENKO and GOODIER, 1951, p. 56). Because the stress trajectory pattern depends upon the deviatoric stress and not the mean stress, an arbitrary pressure may be added over the entire region without changing the results.

One of the solutions treats the stock at West Peak as a pressurized cylindrical hole (source) of radius, r_0, in an infinite two dimensional sheet with no stress at infinity. A constant normal stress and zero shear stress are applied on the hole boundary. The stress function for this geometry is $\Phi_s = A_1 \ln r_1$, where r_1 is the radial coordinate centered inside the hole (TIMOSHENKO and GOODIER, 1951, pp. 55–60). Because the radial stress equals the pressure, P, at $r_1 = r_0$ we must have $A_1 = Pr_0^2$ to satisfy the boundary condition. The mechanical effects produced by structures paralleling the Sangre de Cristo mountain front are treated by superimposing another pressurized cylindrical hole (image) at a distance of 2 d, twice that from West Peak to the mountain front. The stress function for the image is $\Phi_i = A_2 \ln r_2$ where r_2 is centered at the image hole. If the two holes have the same radius and pressure. $A_2 = Pr_0^2$. For the source-image system with uniform internal pressure the stress function is $\Phi_{si} = Pr_0^2 \ln r_1 r_2$.

Superposition of the image stresses in this manner results in only an approximate solution to the problem. The desired boundary conditions on the source are not satisfied. The shear stress will not be zero; the normal stress will not be a constant equal to P; and the stress trajectories will not be radial. However, if the distance between source and image is large compared to the radii of the holes, these alterations are small and can be ignored. For example, the radial stress induced by uniform pressure in the image is $P(r_0/r_2)^2$. Using distances appropriate for West Peak stock ($r \leq 2.6$ km; $d = 8.1$ km) the pressure on the boundary of the source is altered by less than 4%. With equal hole radii and equal positive pressure in both source and image, all displacements perpendicular to the mirror plane between the source and image cancel. Displacements parallel to the mirror plane do not vanish, but double due to the superposition of the image. The mirror plane is a principal stress trajectory with zero shear stress and thus acts as if it were a lubricated rigid boundary.

We judge from Odé's work that equal pressures in the source and image result in a more satisfactory trajectory pattern than equal magnitudes but opposite sign. To further improve the correspondence between the stress trajectories and the dike pattern, Odé superimposed a homogeneous far field stress system (C, B in Odé's paper; S_1, S_3 in the present paper) which ignores the presence of the source and image. The stress function for a homogeneous stress in an infinite region without holes is $\Phi_f = \frac{1}{2}r^2 S_1 \cos^2\theta + \frac{1}{2}r^2 S_3 \sin^2\theta$. The S_1 direction corresponds to $\theta = 0°$ and is the maximum principal stress. Odé observed that the symmetry axis of the dike

pattern was nearly perpendicular to the long range trend of the Sangre de Cristo range and assumed this indicated that the principal regional stresses acted perpendicular and parallel to the mountain front. He therefore superimposed the far field stresses orthogonal to the rigid boundary by centering the polar coordinates midway between the source and image and letting $\theta = 90°$ correspond to the rigid boundary.

The stress function for the far field stress used by Odé may be modified by replacing θ with $\theta - \phi$ where ϕ is an arbitrary angle between the direction of the maximum principal far field stress, S_1, and the perpendicular to the rigid boundary (Fig. 2). The stress function is

$$\Phi_f = \tfrac{1}{2}S_1 r^2 \cos^2(\theta - \phi) + \tfrac{1}{2}S_3 r^2 \sin^2(\theta - \phi).$$

This modification allows us to vary the orientation of the far field stresses and rigid boundary.

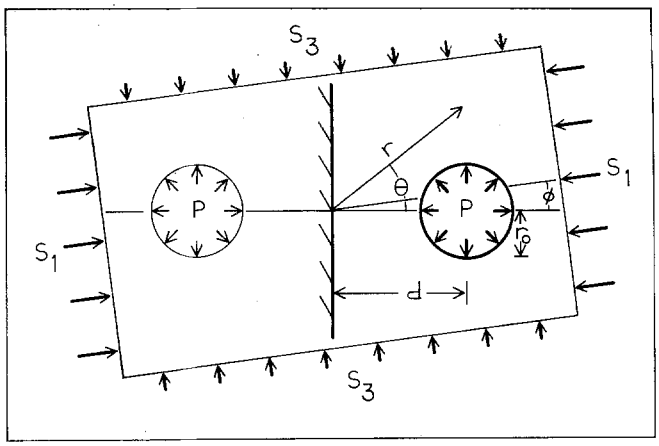

Figure 2
Boundary conditions and parameters used in our model. Two circular holes separated a distance of $2d$, both pressurized with a positive pressure P. The regional stress system, S_1; S_3, is rotated by ϕ from being perpendicular to the rigid boundary. The polar coordinate system is r; θ.

The far field stress is homogeneous throughout the two dimensional sheet and thus alters the desired boundary conditions at the source and along the rigid boundary. We will show below that an appropriate stress trajectory pattern is obtained when $(S_1 - S_3)/P \leq 0.05$. The principal stress difference introduced at the source by the far field stresses is less than 5% of P. We will show below that the boundary conditions along the rigid boundary for distances less than d from the origin are not significantly altered by this superposition. We conclude that this solution is a satisfactory approximation of the solution for the desired boundary conditions.

Differentiating the far field stress function, Φ_f, to obtain the stresses and applying some trigonometric identities we find:

$$(\sigma_{rr})_f = S_3 + (S_1 - S_3)\cos^2(\theta - \phi) \tag{1a}$$

$$(\sigma_{\theta\theta})_f = S_3 + (S_1 - S_3)\sin^2(\theta - \phi) \tag{1b}$$

$$(\sigma_{r\theta})_f = -(S_1 - S_3)\sin(\theta - \phi)\cos(\theta - \phi) \tag{1c}$$

The stresses due to the source image-system are given by:

$$(\sigma_{rr})_{si} = -(\sigma_{\theta\theta})_{si} = Pr_0^2[\xi^6 - \xi^4 d^2 \sin^2\theta - (\xi\, dr)^2\cos^2\theta - d^4r^2\sin^2\theta\cos^2\theta]/[\xi^4 - d^2r^2\cos^2\theta]^2 \tag{2a}$$

$$(\sigma_{r\theta})_{si} = -Pr^2[d^2\sin\theta\cos\theta(\xi^4 - 2\xi^2r^2 + d^2r^2\cos^2\theta)]/[\xi^4 - d^2r^2\cos^2\theta]^2 \tag{2b}$$

Here $2\xi^2 = r^2 + d^2$. Note that the normal stresses are equal but opposite in sign. The total stress field is found by adding (1) and (2). The angle ω made by the maximum principal stress trajectory with the normal to the rigid boundary is given by

$$\omega = \theta + \tfrac{1}{2}\tan^{-1}[2\sigma_{r\theta}/(\sigma_{\theta\theta} - \sigma_{rr})], \quad \sigma_{rr} > \sigma_{\theta\theta} \tag{3a}$$

$$\omega = \theta + \tfrac{1}{2}\pi + \tfrac{1}{2}\tan^{-1}[2\sigma_{r\theta}/(\sigma_{\theta\theta} - \sigma_{rr})], \quad \sigma_{rr} < \sigma_{\theta\theta} \tag{3b}$$

The local principal stress difference is given by:

$$\sigma_1 - \sigma_3 = 2\{[(\sigma_{\theta\theta} - \sigma_{rr})/2]^2 + \sigma_{r\theta}^2\}^{1/2} \tag{4}$$

The equations developed above are formidable, and it is not obvious what effect changing the magnitude, $(S_1 - S_3)/P$, or the orientation, ϕ, of the far field stresses will have on the stress trajectory pattern. This problem can be simplified by noting that each stress trajectory pattern has two unique isotropic stress points where $\sigma_{rr} = \sigma_{\theta\theta}$ and $\sigma_{r\theta} = 0$. It is not difficult to visualize locations of the isotropic points if a pattern of trajectories is known. We construct a map from which values of $(S_1 - S_3)/P$ and ϕ can be found for particular locations of the isotropic points. This provides the capability of using a dike pattern to predict relative magnitude and orientation of the regional stresses.

Figure 3 shows the stress trajectories produced for selected values of $(S_1 - S_3)/P$ and ϕ. Distances are normalized by d and the stress difference is normalized by $P(r_0/d)^2$. The locations of isotropic points relative to stress trajectory patterns are illustrated in this figure. The curvature of the trajectories is greatest near these points and diminishes in every direction as one moves away from them. Trajectories tend to diverge from the isotropic points, whereas they converge radially towards the center of the source. Far from the source the trajectories are parallel to the maximum far field stress (Fig. 3b, c, d). If there is no far field stress the trajectories far from the source are radial to the point midway between the source and image (Fig. 3a). As $(S_1 - S_3)/P$ increases relative to $(r_0/d)^2$, the isotropic points move closer to the

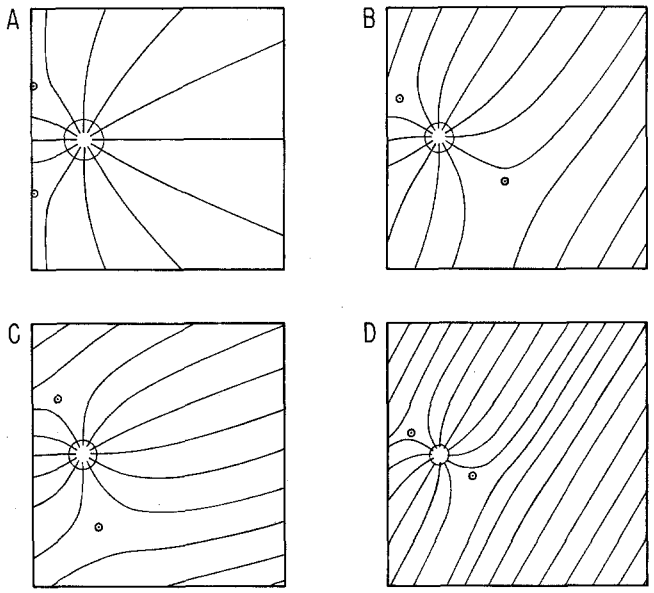

Figure 3
Stress trajectory patterns: The isotropic points for each case are shown, and a circle, centered on the intrusion with a radius of one third the distance to the nearest isotropic point, demonstrates the maximum hole size permitted by the postulates in the model. (A) No regional stress. (B) Normalized regional stress difference of 1.0; $\phi = 60°$. (C) Normalized regional stress difference of 1.0; $\phi = 20°$. (D) Normalized regional stress difference of 4.0; $\phi = 60°$.

source (Fig. 3b, d). As ϕ increases and the trajectories rotate in a counter-clockwise fashion, the isotropic points also rotate (Fig. 3b, c). The trajectories are nearly normal to the rigid boundary within a distance, d, of the origin in both Figure 3a, c. Thus addition of this regional stress does not significantly alter the stress trajectories at the rigid boundary.

Given the locations of isotropic points, Fig. 4 may be used to determine the far field stress parameters. First consider the case of a single pressurized circular hole with homogeneous far field stresses. Superposition of Φ_s and Φ_f results in

$$(\sigma_{rr})_{sf} = P(r_0/r)^2 + (S_1 - S_3)\cos^2(\theta - \phi) \tag{5a}$$

$$(\sigma_{\theta\theta})_{sf} = -P(r_0/r)^2 + (S_1 - S_3)\sin^2(\theta - \phi) \tag{5b}$$

$$(\sigma_{r\theta})_{sf} = -(S_1 - S_3)\sin(\theta - \phi)\cos(\theta - \phi) \tag{5c}$$

neglecting a hydrostatic stress which has no effect on the isotropic points. There will be two isotropic points. These lie on a line through the center of the hole in the direction of the minimum principal far field stress and at a distance, r_i, from the center. The normalized distance is

$$r_i/r_0 = \pm[2P/(S_1 - S_3)]^{1/2} \tag{6}$$

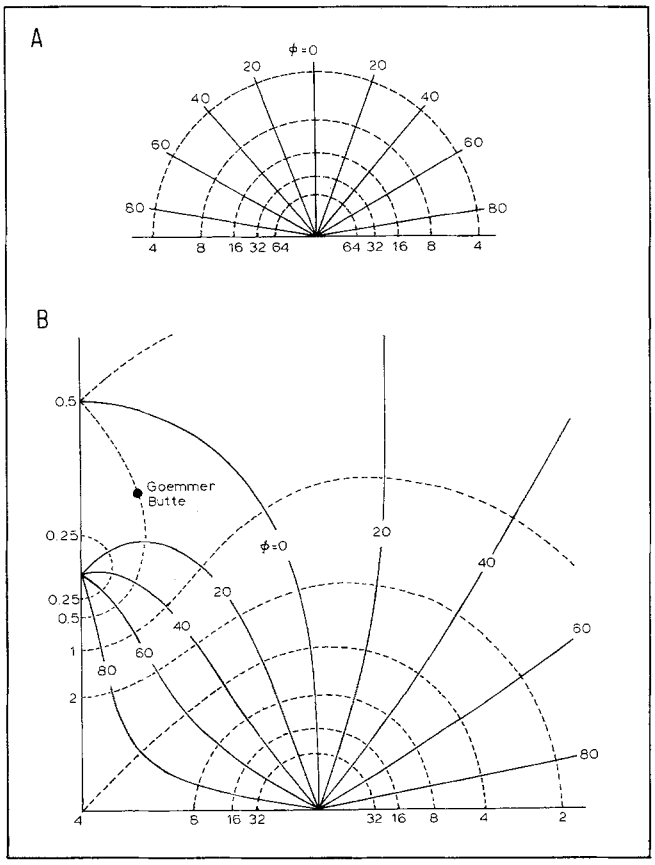

Figure 4
The isotropic point maps. Circumferential numbers refer to the angle made by the regional stress with an east–west line. Numbers along the horizontal axis refer to values for the normalized regional stress. (A) Map for no rigid boundary. (B) Map for our model.

Each possible combination of $(S_1 - S_3)/Pr_0^2$ and ϕ can be associated with a point in Fig. 4a. Lines of constant ϕ are radial and lines of constant $(S_1 - S_3)/Pr_0^2$ are circular. Given r_i/r_0 the relative stresses are determined.

In the case of an image with equal pressure located a distance, $2d$, from the source, the picture is more complicated. In Fig. 4b the hole radius, r_0, is normalized by d and the far field stress difference is normalized by Pr_0^2/d^2. Curves of constant ϕ and constant $(S_1 - S_3)d^2/Pr_0^2$ are shown. Given the locations of the isotropic points as well as r_0 and d the relative stresses are determined.

The following restrictions are put on the use of Fig. 4 in order to approximate the desired boundary conditions at the source. For the source-image system the radius of the source must be less than about $0.4d$ to avoid alteration by the image. There is a limit to the source radius beyond which the trajectories at the boundary are signifi-

cantly non-radial. We choose a limit such that r_0 is less than one third the distance to the closer isotropic point. A consequence of these restrictions is that $(S_1 - S_3)/P$ must be less than 0.2.

4. Interpretation of the Dike Pattern

Because of detailed maps and some relative and absolute age dates now available (JOHNSON, 1968; SMITH, 1975, 1976) a selection of dikes (Fig. 1) can be made. Smith dated several radial dikes at 20 to 25 million years. We eliminate the older, sub-parallel, east-trending dikes and divide the radial dikes according to Johnson's petrologic identification.

Those of syenite and syenodiorite composition are chosen to compare with the model for several reasons. They are numerous and clearly represented in all quadrants around the peak. Thus we will have sufficient data to compare with the model and can determine the correlation on all sides of the peak. These two petrologic types are considered by Johnson, on the basis of dike intersections, to have been intruded sequentially. Therefore selecting dikes of these two closely associated compositions increases the likelihood that we are dealing with a time span during which the regional and local stresses did not vary substantially. That this is not strictly true is evidenced by syenodiorite dikes among the subparallel set. Those dikes not used in the analysis are shown in Fig. 1a in which the subparallel syenodiorite dikes appear as the thicker lines.

We now establish the orientation of the rigid boundary. Odé observed that the dike pattern on Knopf's map was roughly symmetrical on both sides of an axis trending N75E, which is nearly perpendicular to the long range trend of the mountain front and the Paleozoic–Mesozoic contact. His use of a line oriented N15W as a rigid boundary followed from this observation. On Fig. 1b this symmetry is not apparent west of West Peak where the dikes tend to be symmetrical about an E–W axis. Most of the dikes west of West Peak on Fig. 1b are absent from Knopf's map and thus were not included in Odé's analysis. Figures 3a, b, c indicate that for relatively small values of $(S_1 - S_3)/P$ or ϕ, stress trajectories between the source and rigid boundary are nearly symmetrical about an axis perpendicular to the boundary and running through the source. The orientations of these trajectories are primarily controlled by the source and boundary rather than the far-field stress. This suggests that the rigid boundary should be oriented N–S.

In addition to the pattern produced by the orientation of dikes on the map, there is the pattern produced by the density of these dikes. On Knopf's map these two patterns are both roughly symmetrical along N75E. On Figure 1b the pattern produced by the areal density of dikes near West Peak is nearly symmetrical along an E–W axis. This is apparent when the dike areal density is contoured. (Fig. 5a.) The orientation of the rigid boundary of the model could be responsible for this east–west symmetry.

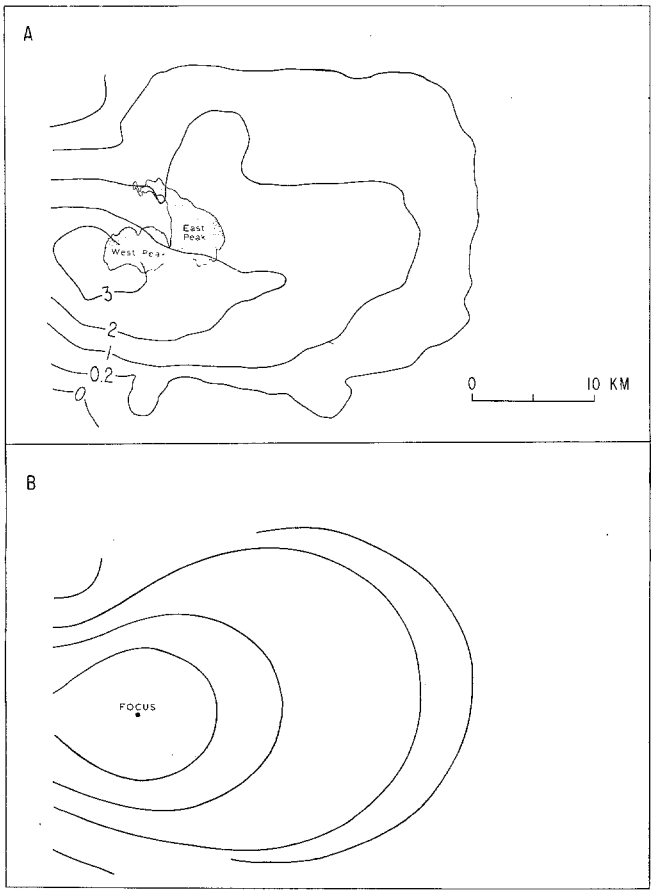

Figure 5
Relationship between dike areal density and local principal stress difference. (A) Areal dike density (number of dikes per 1.27 km^2 averaged over 62 km^2). (B) Contours of one half the local principal stress difference calculated for $\phi = 8°$; $d^2(S_1 - S_3)/Pr_0^2 = 0.5$.

We suggest that the local principal stress difference is related to dike areal density. A region having great principal stress difference could accommodate more dikes than a region having less principal stress difference. Figure 5b is a contour map of the local principal stress differences for the model determined using equation (4). We show below that values of the ratio $(S_1 - S_3)d^2/Pr_0^2$ of about 0.5 produce patterns similar to Fig. 1b. With ratios this small, very little effect is seen in the symmetry of the principal stress difference plot near the source, regardless of the values chosen for ϕ. Thus the dike areal density near West Peak should be relatively insensitive to the orientation of the regional stress and should be a good indicator of the orientation of the rigid boundary. The east–west symmetry near West Peak apparent in Fig. 5a suggests that the rigid boundary should be oriented N–S.

After locating one of the isotropic points we can use Fig. 4 to determine regional stress parameters. The principal stress difference is zero at an isotropic point; hence, an isotropic point should occur where the dike areal density is least. Figures 1b and 5a indicate probable locations near the mountain front northwest and southwest of West Spanish Peak. In the northern region there is a small syenodiorite intrusion, Goemmer Butte, with steep contacts and nearly circular plan. An intrusion with circular plan is not unexpected in a region having a small principal stress difference. We arbitrarily choose Goemmer Butte as one isotropic point.

We now determine the distance, d, between the source and a north–south rigid boundary. Several structures with this orientation lie west of the western termination of the dikes. These include the White Mountain intrusion, the strike of the upturned Mesozoic strata, and the contact between these strata and the intensely folded and faulted Paleozoic rocks. Any of these structures might be responsible for an abrupt increase in the elastic moduli in the horizontal plane. Such an increase would produce mechanical effects similar to the zero displacement boundary condition. A soft bed or bedding planes with low shear strength within the upturned Mesozoic strata could

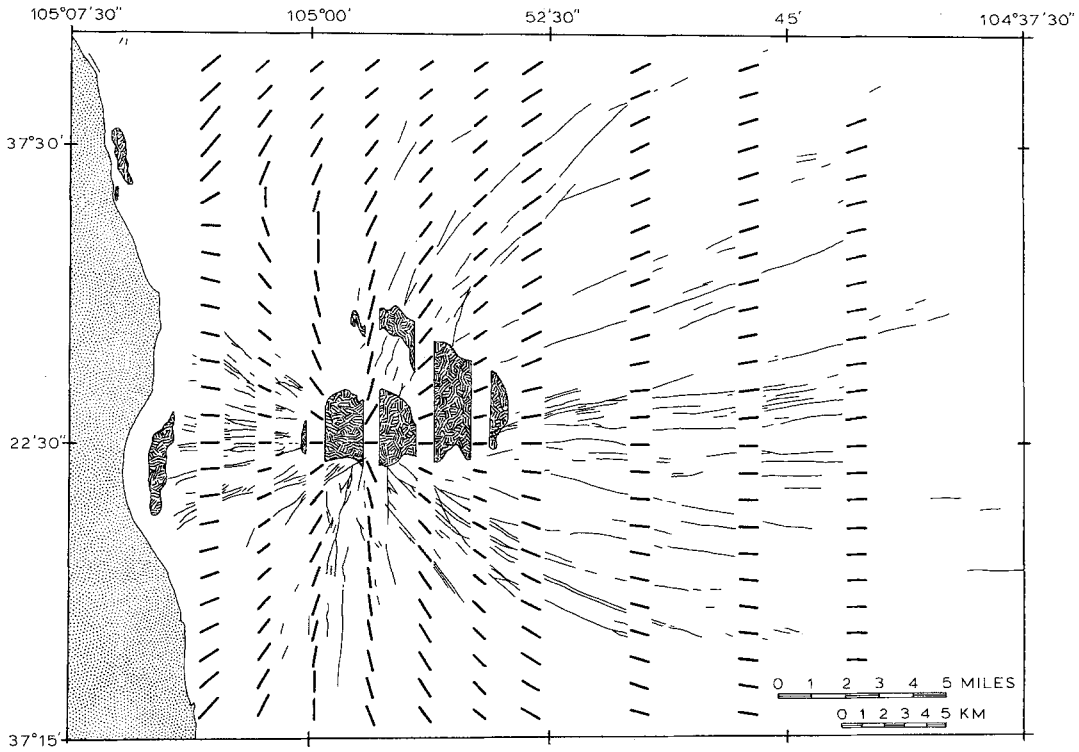

Figure 6
Map of calculated stress trajectories (short, thick lines) and the dikes used in our analysis (thin lines). Trajectories and dikes are presented in alternating strips across the map to facilitate correlation.

reduce the transmitted shear stress. This would produce mechanical effects similar to the zero shear stress boundary condition. ERDOGAN and BIRICIKOGLU (1973) investigated the propagation of a pressurized crack approaching a boundary with a material of greater modulus. The crack tip stress intensity falls abruptly toward zero near the boundary suggesting that crack propagation might cease just before the boundary. For this reason we locate the rigid boundary along the western termination of the dikes. The distance, d, from the rigid boundary to the focal point of the dikes (i.e., the center of the West Peak intrusion) is about 8 km.

The origin of polar coordinates $(r:\theta)$ is at the intersection of the rigid boundary and an east–west line through the focal point. In polar coordinates the location of the isotropic point (Goemmer Butte) is $r = 11$ km; $\theta = 79°$. From these data and Fig. 4b we find that $\phi = 8°$ and $d^2(S_1 - S_3)/Pr_0^2 = 0.5$. Because the rigid boundary is north–south this value of ϕ yields an orientation of the maximum principal regional stress of N82E. We now have values for all parameters necessary to compile a stress trajectory map. The maximum principal stress trajectories and the dikes used in the analysis are shown together in Figure 6. The correlation is excellent.

5. *Discussion*

In the preceding analysis we employed three basic assumptions: (1) linear elasticity is an appropriate theory for conditions in the Spanish Peaks region during dike emplacement; (2) a pressurized, circular hole, a rigid, planar boundary and uniform regional stresses adequately describe the boundary conditions; (3) dikes were emplaced along a unique set of trajectories of maximum principal stress. Geological and mechanical arguments were used to position the rigid boundary along a N–S line about 8 km west of the focus of the radial dike system. Goemmer Butte was selected as a point of isotropic stress. With this information we used the model to deduce a maximum regional principal stress direction of N82E and a value of 0.5 for the ratio $(S_1 - S_3)\, d^2/Pr_0^2$. This stress state was active in the Spanish Peaks region between 20 and 25 million years ago.

By estimating the source radius, r_0, the ratio of the regional stress difference to the pressure in the source can be calculated. A radius of 2.6 km circumscribes the exposed igneous complex near West Peak as well as the two focal areas identified by SMITH (1975). This seems like a reasonable upper limit for the radius, and results in an upper limit for the regional stress difference of $(S_1 - S_3) = 0.05P$. The radius of Smith's smaller focal area is about 0.5 km which yields $(S_1 - S_3) = 0.002P$. We cannot determine precisely the radius at the time of intrusion of syenite and syenodiorite dikes from geological observations, because considerable enlargement of the conduit may have occurred during subsequent magma movement, and the surface radius may be significantly different from that at depth.

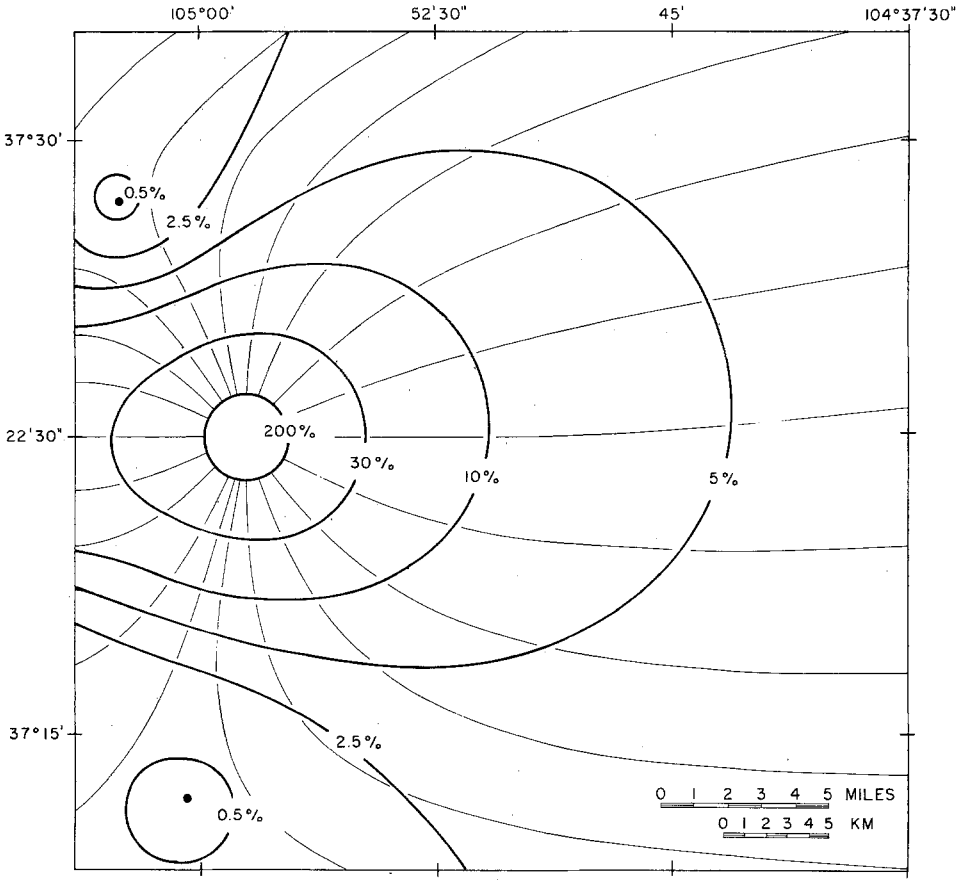

Figure 7
Local principal differences and trajectories of the maximum principal stress. The bold lines contour the stress difference as a percentage of P for the case $r_0 = 2$ km, $\phi = 8°$, and $(S_1 - S_3)\, d^2/Pr_0 = 0.5$. Thinner lines are the stress trajectories and the two solid dots are points of isotropic stress.

For the purpose of further discussion we arbitrarily choose $r_0 = 2$ km and $(S_1 - S_3) = 0.03P$. Figure 7 illustrates the proposed stress state in the horizontal plane covering a region of about 1600 km^2 around the Spanish Peaks. Maximum principal stress trajectories and contours of the local principal stress difference as a percentage of the magma driving pressure are shown. The stress field is very heterogeneous over the region. Trajectories trend in all possible compass directions and the principal stress difference varies by almost two orders of magnitude. It is clear that a few isolated measurements of stress would not adequately characterize the complete stress field. Geological discontinuities along the Sangre de Cristo mountain front and around the West Peak intrusive complex apparently coincide with mechanical discontinuities which significantly altered an otherwise uniform regional stress field. On

the other hand, geological structures such as joints and lithologic layering within the Raton Basin apparently did not influence the stress field strongly at the scale we are considering. Local differences between the trajectory and dike patterns may be attributable to these structures.

To determine the regional principal stress difference we must estimate the magma driving pressure, P. Arguments based on the density contrast between magma and host rock (JOHNSON and POLLARD, 1973) suggest an upper limit of about 100 MN/m^2. A regional stress difference of this magnitude results in a local principal stress difference of 200 MN/m^2 at the boundary of the stock. The ultimate strengths of elastic sedimentary rocks at confining pressures less than 150 MN/m^2 and at high temperatures (HANDIN, 1966) are generally less than 200 MN/m^2, so this appears to be a good upper limit. Using $P \leq 100$ MN/m^2 and $r_0 \leq 2.6$ km we find $(S_1 - S_3) < 5$ MN/m^2. For comparison, BREDEHOEFT *et al.* (1976) report an average value of 2.1 MN/m^2 for the principal stress difference in the horizontal plane in the Piceance Basin, Colorado. They made 26 measurements to depths of 0.5 km in seven different holes using hydraulic fracturing techniques. In light of this data, our predicted upper limit would seem to be quite reasonable for the Raton Basin at the time of dike intrusion.

Acknowledgements

We thank Ross Johnson of U.S.G.S. Denver, Arvid Johnson of Stanford University, and Barry Raleigh and Bill Holman of U.S.G.S. Menlo Park for critically reading the manuscript and offering useful suggestions for its improvement. Richard Smith of Climax Molybdenum Co. generously shared his data and ideas concerning the dikes southeast of West Peak.

REFERENCES

ANDERSON, E. M. (1938), *The dynamics of sheet intrusion*, Proc. Roy Soc. Eding. *58*, no. 3, 242–251.

ANDERSON, E. M., *The Dynamics of Faulting and Dyke Formation with Applications to Britain* (Hafner, New York 1972), 206p.

BIRCH, F., *Compressibility, Elastic Constants* in *Handbook of Physical Constants* (ed. S. P. Clark), The Geol. Soc. of America (New York, 1966), pp. 97–174.

BRACE, W. F. and BOMBOLAKIS, E. G. (1963), *A note on brittle crack growth in compression*, J. Geophys. Res. *68*, 3709–3713.

BREDEHOEFT, F. D., WOLFF, R. G., KEYS, W. S. and SHUTER, E. (1976), *Hydraulic fracturing to determine the regional in situ stress field, Piceance Basin, Colorado*, Geol. Soc. America Bull., *87*, 250–258.

ENDLICH, F. M. (1878), *Report on the Geology of the White River District*, Tenth Annual Report of the U.S. Geological and Geographical Survey of the Territories, 63–131.

ERDOGAN, F. and SIH, G. C. (1963), *On the crack extension in plates under plane loading and transverse shear*, J. Basic Engineering, *85*, 519–527.

ERDOGAN, F. and BIRICIKOGLU, V. (1973), *Two bonded half planes with a crack going through the interface*, Int. J. Engineering Sci., *11*, 745–766.

HANDIN, J., *Strength and ductility*, in Handbook of Physical Constants (ed. S. P. Clark) (The Geol. Soc. of America, New York 1966), 223–290.

HILLS, R. C. (1901), *Description of the Spanish Peaks quadrangle, Colorado*, U.S. Geological Survey Geol. Atlas Folio 71, 70.

HILLS, E. S., *Elements of structural geology* (Wiley, New York 1963), 483 pp.

HOEK, E. and BIENIAWSKI, Z. T. (1965), *Brittle fracture propagation in rock under compression*, Int. J. Fracture Mech. *1*, 137–155.

JOHNSON, A. M., *Physical processes in geology* (Freeman and Cooper, San Francisco 1970), 577 pp.

JOHNSON, A. and POLLARD, D. D. (1973), *Mechanics of growth of some laccolithic intrusions in the Henry Mountains, Utah, 1*, Tectonophysics, *18*, 261–309.

JOHNSON, R. B. (1960), *Brief description of the igneous bodies of the Raton Mesa region, south-central Colorado*, in *Guide to the Geology of Colorado*, Geol. Soc. America, Rocky Mtn. Assoc. Geologists, and Colorado Sci. Soc., 117–120.

JOHNSON, R. B. (1961), *Patterns and origin of radial dike swarms associated with West Spanish Peak and Dike Mountain, south-central Colorado*, Geol. Soc. America Bull. *72*, 579–590.

JOHNSON, R. B. (1968), *Geology of the igneous rocks of the Spanish Peaks region, Colorado*, Geol. Soc. America Bull. *47*, 1727–1784.

KNOPF, A. (1936), *Igneous geology of the Spanish Peaks region, Colorado*, Geol. Soc. America Bull. *47*, 1727–1784.

MUSKHELISHVILI, N. I., *Some Basic Problems of the Mathematical Theory of Elasticity* (Noordhoff, Leyden 1975), 732 pp.

ODÉ, H. (1957), *Mechanical analysis of the dike pattern of the Spanish Peaks area, Colorado*, Geol. Soc. America Bull. *68*, 567–576.

POLLARD, D. D., MULLER, O. H. and DOCKSTADER, D. R. (1975), *The form and growth of fingered sheet intrusions*, Geol. Soc. America Bull. *86*, 351–363.

POLLARD, D. D. (1973), *Derivation and evaluation of a mechanical model for sheet intrusion*, Tectonophysics, *19*, 233–269.

SIH, G. C. (1974), *Strain-energy-density factor applied to mixed mode crack problems*, Int. J. Fracture, *10*, 305–321.

SMITH, R. P. (1973), *Age and emplacement structures of the Spanish Peaks dikes, south-central Colorado*, Geol. Soc. America. Abs. with Programs (Cordilleran Sec.), *5*, 513.

SMITH, R. P. (1975), *Structure and petrology of Spanish Peaks dikes, south-central Colorado*, Ph.D. Thesis, University of Colorado, Boulder, 191 pp.

SMITH, R. P. (1976), *Compositional evolution and tectonic relations of Spanish Peaks igneous rocks, south-central Colorado*, Geol. Soc. America, Abs. with Programs (Rocky Mountain Sec.) *8*, 632.

STEVENS, B. (1911), *The laws of intrusion*, American Inst. of Mining Eng. Bull. *49*, 1–23.

TIMOSHENKO, S. and GOODIER, J. N., *Theory of Elasticity* (McGraw-Hill, New York 1951), 506 pp.

(Received 4th October 1976)